Experimental Animals

Special Field: Pathology

Amyloidosis-inducing Activity of Blood Cells in Mouse AApoAII Amyloidosis

Running head: AMYLOIDOSIS INDUCING ACTIVITY OF BLOOD CELLS

Xin DING[1)], Yingye LIU[1)], Mu YANG[1)], Lin LI[1)], Hiroki MIYAHARA[1)], Jian DAI[1)], Zhe XU[1)], Kiyoshi MATSUMOTO[2)], Masayuki MORI[1,3)], Keiichi HIGUCHI[1,4)], and Jinko SAWASHITA[1,4)]

[1)]*Department of Aging Biology, Institute of Pathogenesis and Disease Prevention, Shinshu University Graduate School of Medicine*, *Matsumoto 390-8621, Japan*

[2)]*Division of Animal Research, Research Center for Supports to Advanced Science, Shinshu University, Matsumoto 390-8621, Japan*

[3)]*Department of Advanced Medicine for Health Promotion, Institute for Biomedical Sciences, Interdisciplinary Cluster for Cutting Edge Research, Shinshu University, Matsumoto 390-8621, Japan*

[4)]*Department of Biological Sciences for Intractable Neurological Diseases, Institute for Biomedical Sciences, Interdisciplinary Cluster for Cutting Edge Research, Shinshu University, Matsumoto 390-8621, Japan*

Address of corresponding authors: K. Higuchi and J. Sawashita, Department of Aging

Biology, Institute of Pathogenesis and Disease Prevention, Shinshu University Graduate School of Medicine, 3-1-1 Asahi, Matsumoto 390-8621, Japan

Abstract: Mouse senile amyloidosis is a disorder in which apolipoprotein A-II (APOA2) deposits as amyloid fibrils (AApoAII) in many organs. We previously reported that AApoAII amyloidosis can be transmitted by feces, milk, saliva and muscle originating from mice with amyloid deposition. In this study, the ability of blood components to transmit amyloidosis was evaluated in our model system. Blood samples were collected from SAMR1.SAMP1-*Apoa2*^{c} amyloid-laden or amyloidosis-negative mice. The samples were fractionated into plasma, white blood cell (WBC) and red blood cell (RBC) fractions. Portions of each were further separated into soluble and insoluble fractions. These fractions were then injected into recipient mice to determine amyloidosis-induction activities (AIA). The WBC and RBC fractions from amyloid-laden mice but not from amyloidosis-negative mice induced AApoAII amyloid deposition in the recipients. The AIA of WBC fraction could be attributed to AApoAII amyloid fibrils because amyloid fibril-like materials and APOA2 antiserum-reactive proteins were observed in the insoluble fraction of the blood cells. Unexpectedly, the plasma of AApoAII amyloidosis-negative as well as amyloid-laden mice showed AIA, suggesting the presence of substances in mouse plasma other than AApoAII fibrils that could induce amyloid deposition. These results indicated that AApoAII amyloidosis could be transmitted across tissues and between individuals through blood cells.

Key Words: amyloidosis, apolipoprotein A-II, blood cells, fibrils, transmission

Introduction

Amyloidosis consists of a group of structural disorders in which normally soluble proteins undergo conformational changes leading to their deposition in tissues as abnormally ordered, insoluble amyloid fibrils [3, 30]. Over 30 different amyloid proteins have been found in human and animal amyloidoses, including amyloid light chain amyloidosis, familial amyloid polyneuropathy and reactive amyloid A amyloidosis [40]. An intriguing feature of the amyloidoses is that they are transmissible. The transmissibility was first demonstrated in prion disease. The transmissible nature of infectious prion protein (PrP^{Sc}) has been demonstrated at 4 levels: (1) direct molecular transmission (self-propagation), (2) spreading within tissue, (3) spreading across tissue and (4) from organism to organism [4]. Subsequently, prion-like transmission was reported in other amyloidoses, such as inflammation-associated AA amyloidosis, Alzheimer's disease and progressive neurodegenerative diseases in mice and other animal species [4, 21, 28, 32, 46].

In order to reduce the prevalence of amyloidoses, it is essential to elucidate the mechanisms of development and progression. Previous studies have demonstrated the importance of blood and its components, including monocytes, platelets, and plasma, as agents for progression and transmission of the diseases. Prion infectivity can reside in the blood of sheep and humans [4, 19]. Furthermore, prions were transmitted by animal blood transfusion prior to the clinical onset of the disease in deer [20, 29]. In mouse amyloidosis models, AA amyloidosis could be transmitted by peripheral blood monocytes [41]. Also, intraperitoneally injected amyloid β (Aβ) fibrils could be detected in blood monocytes in a transgenic mouse model of Alzheimer's disease [5]. Supposedly, these cells transport Aβ seeds from the periphery to the

brain where they induce cerebral Aβ amyloidosis. Blood platelets express the amyloid precursor protein (APP) and enzymatic machinery to process APP proteins into Aβ peptides. Furthermore, platelets can transform soluble Aβ into fibrillar structures, absorb Aβ fibrils and accumulate in amyloid deposits in cerebral vessels [10]. Recently, transmissible spongiform encephalopathy-associated prion protein (PrP^{TSE}) has been demonstrated in extracellular vesicle preparations containing exosomes from the plasma of mice infected with mouse-adapted variant Creutzfeldt-Jakob disease [37]. Still, much remains to be done to understand the molecular mechanism of propagation and transmission of amyloidosis.

Mouse senile amyloidosis is a disorder in which apolipoprotein A-II (APOA2) of plasma high-density lipoprotein deposits as amyloid fibrils (AApoAII) in many organs [18, 42]. In inbred strains of mice, 6 alleles (*a, b, c, d, e* and *f*) of the APOA2 gene (*Apoa2*) have been found [24]. AApoAII amyloidosis is observed frequently in aged mice of various strains with these alleles. During aging, strains with the *Apoa2*^{c} allele in particular exhibit a high incidence of severe spontaneous systemic amyloid deposits [12, 15, 17, 39].

SAMR1.SAMP1-*Apoa2*^{c} (R1.P1-*Apoa2*^{c}) mice constitute a congenic strain with the amyloidogenic *Apoa2*^{c} allele of the SAMP1 strain on the genetic background of SAMR1 mice. This strain exhibits a high incidence of AApoAII amyloidosis, and it has provided a useful system to study the pathogenesis of amyloidosis [16]. We have shown that AApoAII amyloid fibrils act as seeds that induce conversion of the native APOA2 to fibrillar AApoAII assemblies *in vitro* [33, 38]. In addition, intravenous injection of a small amount of an AApoAII amyloid fibril fraction extracted from various organs of amyloid-laden mice into young R1.P1-*Apoa2*^{c} mice readily induces AApoAII amyloidosis [13, 26, 47]. Transmission

of AApoAII amyloidosis through feces and from mother to babies through milk has also been demonstrated in R1.P1-*Apoa2*^{c} mice [25, 43]. Thus, mouse AApoAII amyloidosis could be transmitted through a seeding mechanism similar to that of infectious prion diseases and other amyloidoses [36, 43].

In this study, we examined whether amyloid deposition could be induced by blood cells of mice with AApoAII amyloidosis using the R1.P1-*Apoa2*^{c} mouse model. We demonstrated amyloidosis-inducing activities (AIA) in the white blood cell (WBC) and red blood cell (RBC) fractions of AApoAII amyloid-laden mice.

Materials and Methods

Animals

We used R1.P1-*Apoa2*^{c} mice that were developed in our laboratory. *Apoa2* knockout mice (*Apoa2*$^{-/-}$) were purchased from Jackson Laboratories. A SAMR1-*Apoa2*$^{-/-}$ (R1-*Apoa2*$^{-/-}$) congenic strain was established by introducing the *Apoa2*$^{-/-}$ allele into the SAMR1 strain by a standard backcross procedure in our laboratory. We confirmed that APOA2 protein was absent in R1-*Apoa2*$^{-/-}$ mice by Western blotting analysis (**Supplementary Fig. S1**). Mice were maintained at the Division of Animal Research, Research Center for Support of Advanced Science, Shinshu University under specific pathogen-free conditions at 24 ± 2 ˚C with a light-controlled regimen (12-h light/dark cycle). A commercial diet (MF; Oriental Yeast, Tokyo, Japan) and tap water were provided *ad libitum*. Only female mice were used in this study to avoid AA amyloidosis or other adverse impacts caused by fighting or other aggressive behavior among male mice reared in the same cage. All experiments were

performed with the approval of the Committee for Animal Experiments of Shinshu University (Approval No: 250023 and 280014).

Preparation of donor mice with and without AApoAII amyloid deposition

The AApoAII amyloid fibril fraction was an aqueous suspension of fibrils isolated from the livers of 13-month-old R1.P1-*Apoa2*^{c} mice as described previously [43] (**Supplementary Fig. S2**). Amyloid fibrils were resuspended at a concentration of 1.0 mg/mL in distilled water (DW). Sonicated amyloid fibrils (100 μg) were then injected into the tail vein of 2-month-old R1.P1-*Apoa2*^{c} mice to induce AApoAII amyloidosis [13]. Two, 4, 7 and 10 months after the injection, 3 mice were sacrificed by cardiac puncture under isoflurane anesthesia and blood was collected in tubes containing heparin. Three R1.P1-*Apoa2*^{c} mice without AApoAII injection were sacrificed at 12 months of age. Blood was collected from these mice and used as an AApoAII amyloid-free control. Three R1-*Apoa2*$^{-/-}$ mice without AApoAII injection were sacrificed at 2 months of age. Blood collected from these mice was used as APOA2-free material.

Organs were then taken from mice and fixed in 10% neutral buffered formalin, embedded in paraffin and cut into serial 4-μm sections. Amyloid deposition was evaluated in Congo red-stained sections by polarizing microscopy. The degree of AApoAII deposition in 7 organs (heart, liver, spleen, stomach, small intestine, tongue and abdominal skin) was determined using an amyloid score (AS) that was graded from 0 to 4 as described previously [44]: grade 0, no AApoAII deposition; grade 1, a minute amount; grade 2, small amounts; grade 3, a moderate amount and grade 4, extensive AApoAII deposition. The degree of AApoAII

deposition in mice was expressed as the amyloid index (AI), which was the average of the AS grades in 7 organs. The identity of the deposited amyloid fibril proteins in organs was verified by immunohistochemical analyses using an avidin-biotin horseradish peroxidase complex method with specific antisera against mouse AApoAII and mouse AA [14].

Separation and processing of plasma, WBC and RBC fractions

Plasma was isolated from whole blood by centrifugation for 20 min at 3,000 x g at 4°C. Blood cell fractions were then separated into the WBC and RBC fractions through use of Lymphocyte M (Mouse) (Cedarlane, Burlington NC) according to the manufacturer's instructions. The cells in the fractions were enumerated with a cell counting chamber (Erma, Tokyo, Japan). After 3 PBS washing steps, the WBC and RBC fractions did not contain plasma and WBCs were not found in the RBC fractions but some amounts of RBCs were found in the WBC fractions (**Supplementary Fig. S3**). Although the majority of WBCs in the WBC fraction consisted of lymphocytes and monocytes with only traces of granulocytes but considerable amounts of RBCs (~50%) were contained. Separated blood components were stored at -70°C until use.

For Western blotting and electron microscopic analyses, WBC, RBC and plasma fractions collected from 9-month-old AApoAII amyloid-laden R1.P1-*Apoa2*^{c} mice were pooled. The protein content of the fractions was determined with the BCA assay (Pierce BCA Protein Assay Kit, Thermo Scientific, Tokyo, Japan). Parts of the pooled components were denatured (1.0 mg/mL) in a solution of 6 M guanidine hydrochloride (GdnHCl), 0.1 M Tris-HCl (pH. 10.0), 50 mM dithiothreitol for 24 h at room temperature. Denatured samples

were dialyzed against DW to remove GdnHCl and subjected to freeze-drying (FD-5N, EYELA Co, Tokyo Japan). The freeze-dried samples, corresponding to 20 μL volumes of the original RBC, WBC or plasma fractions, were dissolved in 100 μL PBS just prior to use.

Portions of the pooled RBC and WBC fractions from 9-month-old AApoAII amyloid-laden R1.P1-*Apoa2*^{c} mice were homogenized in PBS using a Power Masher (Nippi Co, Tokyo, Japan). Homogenates were then subjected to centrifugal fractionation. Homogenates were first centrifuged at 3,000 x g for 5 min at 4°C. Supernatants were transferred to new tubes and the sediment was resuspended in PBS (3KG-P fraction). The supernatants were centrifuged at 100,000 x g for 1 h at 4°C. The supernatants were transferred to new tubes (Sol fraction) and the sediments were resuspended in PBS (100KG-P fraction).

Determination of the AIA of blood components

Samples consisted of WBC, RBC or plasmas fractions (20 μL per fraction) (**Table 1**), or processed blood components (3KG-P, 100KG-P, Sol and GdnHCl treated fractions) were diluted with PBS to 100 μL, and injected into the tail veins of 3 two-month-old R1.P1-*Apoa2*^{c} recipient mice. Two months after injection, the recipient mice were sacrificed, and the degree of amyloid deposition (AI) was measured using the methods detailed above. The AIA of each sample was determined as the mean AI value across the 3 recipient mice.

Western blotting and ultrastructural analyses

Western blotting analysis was performed using Tris-Tricine/SDS-16.5% polyacrylamide gels (SDS-PAGE). Proteins in the WBC fraction separated with SDS-PAGE were transferred

to polyvinylidene difluoride membranes (Bio-Rad Laboratories, Hercules, CA). The membrane was incubated with polyclonal rabbit anti-mouse APOA2 antiserum [14] and reacted proteins were detected with the enhanced chemiluminescence method (Amersham Biosciences, Buckinghamshire, England) with X-ray film (Amersham Biosciences). The negatively stained 3KG-P, 100KG-P and Sol fractions of pooled WBC fraction from 9-month-old amyloid-laden R1.P1-*Apoa2*^{c} mice were observed with a JEM-1400 electron microscope (JEOL, Tokyo, Japan) with an acceleration voltage of 80 kV [46].

Statistical Analysis

Statistical analysis was performed with SPSS (Abacus Concepts, Berkley, CA) and R software (The R Development Core Team, Vienna University of Economics and Business, Vienna, Austria). For non-parametric statistical analysis of AI of recipient mice injected with each sample, we applied the Kruskal-Wallis test followed by the Steel-Dwass test for adjusting multiple comparisons.

Results

AApoAII amyloid deposition in donor mice

In order to prepare blood that could harbor AIA, AApoAII amyloidosis was induced in 2-month-old R1.P1-*Apoa2*^{c} mice by administration of AApoAII amyloid fibrils. The mice were sacrificed at 4, 6, 9 and 12 months of age. The degree of AApoAII amyloid deposition increased with age in each organ. Accordingly, the AI of the mice increased from 1.56 (mean of 3 mice) at the age of 4 months to 2.76 (6 months), 2.95 (9 months) and 3.09 (12 months)

(**Fig. 1**). Amyloid deposition was not observed in any organs in 12-month-old R1.P1-*Apoa2*^{c} or 2-month-old R1-*Apoa2*$^{-/-}$ mice that were not administered AApoAII fibrils. Using immunohistochemical staining with anti-mouse AApoAII and AA antisera, we confirmed that amyloid deposition was AApoAII and not AA, which is a major amyloid deposit associated with inflammation. These results indicated that these mice could be used as blood donors to evaluate their AIA.

The WBC and RBC fractions from AApoAII amyloid-laden mice had AIA

Both the WBC and RBC fractions collected from the AApoAII amyloid-laden mice showed AIA. It was expected that the WBC and RBC fractions collected from older mice with more severe AApoAII amyloid deposition would have higher AIA. Contrary to this expectation, the mean AIA values of the WBC fractions collected from mice at the ages of 4 (0.43), 6 (0.57), and 9 months (0.84) were not statistically different. AIA values of the WBC fractions collected from 12-month-old mice (0.35) were significantly lower than those of the WBC fractions from 9-month-old mice (**Fig. 2A and C**). AIA values of the WBC fractions from AApoAII amyloidosis-negative R1.P1-*Apoa2*^{c} and R1-*Apoa2*$^{-/-}$ mice were virtually undetectable, with mean values of 0.02 and 0.00, respectively. Injection of PBS to recipient mice did not induce amyloid deposition (AIA = 0). The AIA values in the WBC fractions of amyloid-laden mice were significantly higher than those in mice without amyloid deposition.

Mean AIA values of RBC fraction collected from AApoAII amyloid-laden mice at the ages of 4, 6, 9 and 12 months were 0.33, 0.27, 0.45 and 0.35, respectively (**Fig. 2B**). AIA values of the RBC fraction collected from amyloidosis-negative R1.P1-*Apoa2*^{c} and

R1-*Apoa2*$^{-/-}$ mice were virtually undetectable, with mean values of 0.00 and 0.05, respectively.

Plasmas from both AApoAII amyloid-laden and amyloidosis-negative mice had AIA

The mean AIA values of plasmas collected from AApoAII amyloid-laden mice at the ages of 4, 6, 9 and 12 months were 0.40, 0.48, 0.67 and 0.49, respectively. There was no significant difference between these values (**Fig. 3A and B**). Plasma collected from AApoAII amyloidosis-negative R1.P1-*Apoa2*^{c} and R1-*Apoa2*$^{-/-}$ mice showed similar AIA values with mean values of 0.32 and 0.66, respectively.

Characterization of amyloidosis-inducing factors in mouse blood cells and plasma

GdnHCl treatment of the WBC, RBC and plasma fractions collected from 9-month-old AApoAII amyloid-laden R1.P1-*Apoa2*^{c} mice completely abolished their AIA (**Table 2**).

The WBC and RBC fractions of 9-month-old AApoAII amyloid-laden R1.P1-*Apoa2*^{c} mice were fractionated into insoluble (3KG-P), 100,000 x g sediment (100KG-P) and soluble (Sol) fractions. AIA was detected in the 3KG-P fraction from the WBC and RBC fractions, but not in the soluble fractions from either WBC or RBC fraction (**Fig. 4, Supplementary Table S1**).

Amyloid fibril-like structures were observed by electron microscopy in the 3KG-P fraction of the WBC fraction from 9-month-old AApoAII amyloid-laden R1.P1-*Apoa2*^{c} mice (**Fig. 5A**). The fibrils from WBC fraction differed in appearance from those in the liver (**Supplementary Fig. S2**), exhibiting much thinner, smaller and noodle-like fibrils

resembling the fibrils from milk [25], muscle [36] and feces [32, 46]. In contrast, such structures were not observed in either the 100kG-P or the Sol fractions from the amyloid-laden mice or any fraction from amyloidosis-negative R1-*Apoa2*$^{-/-}$ mice.

We conducted Western blotting analyses of the 3 fractions of WBC fractions from 9-month-old AApoAII amyloid-laden R1.P1-*Apoa2*^{c} and amyloidosis-negative R1-*Apoa2*$^{-/-}$ mice using anti-mouse APOA2 antiserum. The study revealed specific bands of ~7 kDa (monomers) and ~15 kDa (dimers) in the 3KG-P fraction and a band of ~15 kDa in the 100KG-P fraction of WBC fraction isolated from the amyloid-laden mice (**Fig. 5B**), but not in the 3KG-P fraction from amyloidosis-negative mice (**Fig. 5C**).

Discussion

In this paper, the ability of blood components to transmit amyloidosis (AIA) was evaluated with the mouse AApoAII amyloidosis model. The study showed that the WBC and RBC fractions of AApoAII amyloid-laden mice harbored AIA, and accordingly could induce AApoAII amyloidosis when transfused into recipient mice. These findings reinforce the notion that blood can transmit amyloidosis.

In previous studies, we demonstrated that AApoAII amyloid fibrils can act as seeds, inducing the conversion of native APOA2 to fibrillar AApoAII assemblies [33, 38]. We also revealed that AApoAII amyloidosis could be induced in young mice by intravenous injection of small amounts of AApoAII amyloid fibril fractions extracted from organs of amyloid-laden mice [13, 26, 47]. In this study, AIA was detected in the insoluble fractions of WBC, RBC and plasma fractions and GdnHCl treatment of the samples abolished the AIA. In addition,

amyloid fibril-like structures and anti-APOA2 reactive bands were detected in the insoluble fraction of WBC fraction. These results suggest that AApoAII amyloid fibrils in the WBC and RBC fractions were responsible for their AIA. It seems likely that the injected AApoAII fibrils were taken up by the WBCs and RBCs in circulation, as these cells do not express APOA2 [8] (BIO GPS. http://biogps.org). However, it is known that blood and monocytes transmit prion disease and mouse AA amyloidosis [19, 20, 27, 29, 41]. It was previously shown in mouse AA amyloidosis [34] and transthyretin transgenic mice [6] that monocytes/macrophages phagocytized amyloid fibrils, leading to partial clearance of amyloidosis. It is possible that the phagocytosis of AApoAII amyloid fibrils by monocytes/macrophages contributed to the transmission of amyloidosis when the cells were transfused to recipients. Tissue cells could be damaged by endocytosis of amyloid fibrils in various amyloidoses [22, 35]. Also, Aβ was demonstrated to bind to RBCs [23]. Thus, it is also possible that cell debris and AApoAII amyloid fibrils of damaged cells bound to the WBCs and RBCs that subsequently transmitted amyloidosis. AIA values of the WBC fraction tended to increase until 9 months of age, but decreased significantly in 12-month-old mice (**Fig. 2A**). The mechanism of the decrease is not clear, but the activity and number of monocyte/macrophages that phagocytize amyloid might decrease with aging along with severe amyloid deposition in the organs of mice [11]. In these experiments, the WBC fractions contained considerable amounts of RBCs, we need further studies to identify which cells are the most responsible for transmission. It remains unclear, however, how the AApoAII amyloid fibrils in or on blood cells interact with precursor APOA2 protein in circulating HDL to convert it to fibrillar AApoAII.

Unexpectedly, AIA was observed in plasma of AApoAII amyloidosis-negative as well as amyloid-laden mice. The identity of the agents with AIA and the mechanisms by which normal plasma induces AApoAII amyloidosis are not apparent. The observation that even plasma of R1-*Apoa2*$^{-/-}$ mice, which were deficient in APOA2 production, induced AApoAII amyloidosis in recipient mice indicated that the substance was something other than AApoAII amyloid fibrils. The finding that the AIA of plasma was abolished after GdnHCl treatment suggests that the unidentified substance with AIA in mouse plasma consisted of peptides with an amyloid fibril-like structure or protein aggregates. We have previously reported that injection of fibril fractions extracted from muscles of mice that were free of AApoAII amyloid deposition could induce AApoAII amyloidosis in recipient mice, although these fractions contained no APOA2 [36]. It is known that mouse AApoAII amyloid can be seeded by various heterogeneous amyloid fibrils (cross-seeding) [9, 45]. Many kinds of proteins form amyloid fibril-like structures [7, 31]. There is a possibility that the substances with amyloid fibril-like structures in the plasma cross-seeded with the APOA2. In the mouse AA amyloidosis model, amyloidosis-enhancing activity was demonstrated in the spleen, liver, kidney and heart tissues from normal mice [1, 2]. These observations suggest that substances other than amyloid fibrils could also induce amyloid deposition. Identification of the substances with AIA in plasma awaits further study.

In summary, the data obtained in this study indicated that the WBC and RBC fractions of AApoAII amyloid-laden mice harbored AIA. Still, much remains to be done to fully understand the pathogenesis of AApoAII and other amyloidoses, in particular the molecular mechanism of transmission and propagation of amyloidosis. Mouse AApoAII amyloidosis

provides useful guidance in determining the pathogenesis of amyloidosis and developing effective preventive treatments.

Acknowledgements

This research was supported by Grants-in-Aid for Scientific Research (B) 17H04063 and 26293084, and Challenging Exploratory Research 26670152 from the Ministry of Education, Culture, Sports, Science, and Technology of Japan and by grants from the Intractable Disease Division, the Ministry of Health, Labor, and Welfare to the Research Committees for Amyloidosis. We thank Dr. Takahiro Yoshizawa and Ms. Kayo Suzuki (Research Center for Supports to Advanced Science, Shinshu University) for the care of mice and technical assistance.

References

1. Axelrad, M.A., Kisilevsky, R., Willmer, J., Chen, S.J., and Skinner, M. 1982. Further characterization of amyloid-enhancing factor. *Lab. Invest*. 47: 139-146.
2. Baltz, M.L., Caspi, D., Hind, C.R.K., Feinstein, A., and Pepys, M.B. Isolation and characterization of amyloid enhancing factor (AEF). In: Glenner GG, Osserman EF, Benditt EP, Calkins E, Cohen AS, Zucker-Franklin D (eds) Amyloidosis. 1986. New York, Plenum Press, pp 115-121.
3. Buxbaum, J.N., Reinhold. P., and Linke, A. 2012. Molecular History of the Amyloidoses. *J. Mol. Biol*. 421: 142–159.
4. Eisele, Y.S., and Duyckaerts, C. 2016. Propagation of Aβ pathology: hypotheses, discoveries, and yet unresolved questions from experimental and human brain studies. *Acta. Neuropathol.* 131: 5-25.
5. Eisele, Y.S., Fritschi, S.K., Hamaguchi, T., Obermüller, U., Füger, P., Skodras, A., Schäfer, C., Odenthal. J., Heikenwalder, M., Staufenbiel. M., and Jucker, M. 2014. Multiple factors contribute to the peripheral induction of cerebral β-amyloidosis. *J. Neurosci.* 34: 10264-10273.
6. Ferreira. N., Gonçalves, N.P., Saraiva, M.J., and Almeida, M.R. 2016. Curcumin: A multi-target disease-modifying agent for late-stage transthyretin amyloidosis. *Sci. Rep*. 6: 26623.
7. Fowler, D.M., Koulov, A.V., Balch, W.E, and Kelly, J.W. 2007. Functional amyloid–from bacteria to humans. *Trends Biochem. Sci*. 32: 217–224.
8. Fu, L., Matsuyama, I., Chiba, T., Xing, Y., Korenaga, T., Guo, Z., Fu, X., Nakayama, J.,

Mori, M., and Higuchi K. 2001. Extrahepatic expression of apolipoprotein A-II in mouse tissues: possible contribution to mouse senile amyloidosis. *J. Histochem. Cytochem*. 49: 739-748.

9. Fu, X., Korenaga, T., Fu, L., Xing, Y., Guo, Z., Matsushita, T., Hosokawa, M., Naiki, H., Baba, S., Kawata, Y., Ikeda S., Ishihara, T., Mori, M., and Higuchi, K. 2004. Induction of AApoAII amyloidosis by various heterogeneous amyloid fibrils. *FEBS Lett*. 563: 179–184.
10. Gowert, N.S., Donner, L., Chatterjee, M., Eisele, Y.S., Towhid, S.T., Münzer, P., Walker, B., Ogorek, I., Borst, O., Grandoch, M., Schaller, M., Fischer, J.W., Gawaz, M., Weggen, S., Lang. F., Jucker, M., and Elvers, M. 2014. Blood platelets in the progression of Alzheimer's disease. *PLoS One.* 9: e90523.
11. Hearps, A.C., Martin, G.E., Angelovich, T.A., Cheng, W.J., Maisa, A., Landay, A.L., Jaworowski, A., and Crowe, S.M. 2012. Aging is associated with chronic innate immune activation and dysregulation of monocyte phenotype and function. *Aging Cell.* 11: 867-875.
12. Higuchi, K., Kitagawa, K., Naiki, H., Hanada, K., Hosokawa, M., and Takeda, T. 1991. Polymorphism of apolipoprotein A-II (apoA-II) among inbred strains of mice: Relationship between the molecular type of apoA-II and mouse senile amyloidosis. *Biochem. J.* 279 (Pt 2): 427–433.
13. Higuchi, K., Kogishi, K., Wang J, Chen X, Chiba T, Matsushita, T., Hoshii, Y., Kawano H., Ishihara, T., Yokota, T., and Hosokawa, M. 1998. Fibrilization in mouse senile amyloidosis is fibril conformation-dependent. *Lab. Invest.* 78: 1535-1542.

14. Higuchi, K., Matsumura, A., Honma, A., Takeshita, S., Hashimoto, K., Hosokawa, M., Yasuhira, K., and Takeda, T. 1983. Systemic senile amyloid in senescence-accelerated mice. A unique fibril protein demonstrated in tissues from various organs by the unlabeled immunoperoxidase method. *Lab. Invest.* 48: 231-240.

15. Higuchi, K., Naiki, H., Kitagawa, K., Hosokawa, M., and Takeda T. 1991. Mouse senile amyloidosis: ASSAM amyloidosis in mice presents universally as a systemic age-associated amyloidosis. *Virchows Arch. B Cell Pathol. Incl. Mol. Pathol.* 60: 231–238.

16. Higuchi, K., Naiki, H., Kitagawa, K., Kitado, H., Kogishi, K., Matsushita, T., and Takeda T. 1995. Apolipoprotein A-II gene, and development of amyloidosis, and senescence in a congenic strain of mice carrying amyloidogenic ApoA-II. *Lab. Invest.* 72: 75-82.

17. Higuchi, K., Wang, J., Kitagawa, K., Matsushita, T., Kogishi, K., Naiki, H., Kitado, H., and Hosokawa, M. 1996. Accelerated senile amyloidosis induced by amyloidogenic ApoA-II gene shortens the life span of mice but does not accelerate the rate of senescence. *J. Gerontol. A Biol. Sci. Med. Sci.* 51: B295-302.

18. Higuchi, K., Yonezu, T., Kogishi, K., Matsumura, A., Takeshita, S., Kohno, A., Matsushita, M., Hosokawa, M., and Takeda, T. 1986. Purification and characterization of a senile amyloid-related antigenic substance (apoSASSAM) from mouse serum. apoSASSAM is an apoA-II apolipoprotein of mouse high density lipoproteins. *J. Biol. Chem.* 261: 12834-12840.

19. Houston, F., McCutcheon, S., Goldmann, W., Chong, A., Foster, J., Sisó, S., González, L., Jeffrey, M., and Hunter, N. 2008. Prion diseases are efficiently transmitted by blood

transfusion in sheep. *Blood.* 112: 4739-4745.

20. Hunter, N., Foster, J., Chong, A., McCutcheon, S., Parnham, D., Eaton, S., MacKenzie, C., and Houston, F. 2002. Transmission of prion diseases by blood transfusion. *J. Gen. Virol.* 83: 2897- 2905.
21. Jucker, M., and Walker, L.C. 2013. Self-propagation of pathogenic protein aggregates in neurodegenerative diseases. *Nature.* 501: 45-51.
22. Kameyama, H., Nakajima, H., Nishitsuji, K., Mikawa, S., Uchimura, K., Kobayashi, N., Okuhira, K., Saito, H., and Sakashita, N. 2016. Iowa mutant apolipoprotein A-I (apoA-IIowa) fibrils target lysosomes. *Sci. Rep*. 6: 30391.
23. Kiko, T., Nakagawa, K., Satoh, A., Tsuduki, T., Furukawa, K., Arai, H., and Miyazawa, T. 2012. Amyloid β levels in human red blood cells. *PLoS One*.7: e49620.
24. Kitagawa, K., Wang, J., Mastushita, T., Kogishi, K., Hosokawa, M., Fu, X., Guo, Z., Mori, M., and Higuchi, K. 2003. Polymorphisms of mouse apolipoprotein A-II: seven alleles found among 41 inbred strains of mice. *Amyloid* 10: 207-214.
25. Korenaga, T., Yan, J., Sawashita, J., Matsushita, T., Naiki, H., Hosokawa, M., Mori, M., Higuchi, K., and Fu X. 2006. Transmission of amyloidosis in offspring of mice with AApoAII amyloidosis. *Am. J. Pathol.* 168: 898-906.
26. Liu, Y., Sawashita, J., Wang, Y., Li, L., Miyahara, H., Ding, X., Yang, M., and Higuchi, K. 2016. Distribution of transmissible amyloid proteins in the liver with apolipoprotein A-II amyloidosis. *Shinshu Med. J.* 64: 183-194.
27. Llewelyn, C.A., Hewitt, P.E., Knight, R.S., Amar, K., Cousens S., Mackenzie, J., and Will, R.G. 2004. Possible transmission of variant Creutzfeldt-Jakob disease by blood

transfusion. *Lancet*. 363: 417-421.

28. Lundmark, K., Westermark, G.T., Nyström, S., Murphy, C.L., Solomon, A., and Westermark, P. 2002. Transmissibility of systemic amyloidosis by a prion-like mechanism. *Proc. Natl. Acad. Sci. U S A*. 99: 6979-6984.
29. Mathiason, C.K., Hays, S.A., Powers, J., Hayes-Klug, J., Langenberg, J., Dahmes, S.J., Osborn, D.A., Miller, K.V., Warren, R.J., Mason, G.L., and Hoover, E.A. 2009. Infectious prions in pre-clinical deer and transmission of chronic wasting disease solely by environmental exposure. *PLoS One*. 4: e5916.
30. Merlini, G., and Bellotti, V. 2003. Molecular mechanisms of amyloidosis.. *N. Engl. J. Med.* 349: 583-596.
31. Münch, J.1., Rücker, E., Ständker, L., Adermann, K., Goffinet, C., Schindler, M., Wildum, S., Chinnadurai, R., Rajan, D., Specht, A, Giménez-Gallego, G., Sánchez, P.C., Fowler, D.M., Koulov, A., Kelly, J.W., Mothes, W., Grivel, J.C., Margolis, L., Keppler, O.T., Forssmann, W.G., and Kirchhoff, F. 2007. Semen derived amyloid fibrils drastically enhance HIV infection. *Cell*.131: 1059–1071.
32. Murakami, T., Ishiguro, N., and Higuchi K. 2014. Transmission of systemic AA amyloidosis in animals. *Vet. Pathol.* 51: 363-371.
33. Naiki, H., Higuchi, K., Nakakuki, K., and Takeda, T. 1991. Kinetic analysis of amyloid fibril polymerization in vitro. *Lab. Invest.* 65: 104-110.
34. Nyström, S.N., and Westermark, G.T. 2012. AA-Amyloid is cleared by endogenous immunological mechanisms. *Amyloid*. 19: 138-145.
35. Okoshi, T., Yamaguchi, I., Ozawa, D., Hasegawa, K., and Naiki, H. 2015. Endocytosed

2-Microglobulin amyloid fibrils induce necrosis and apoptosis of rabbit synovial fibroblasts by disrupting endosomal/lysosomal membranes: a novel mechanism on the cytotoxicity of amyloid fibrils. *PLoS One.* 10: e0139330.

36. Qian, J., Yan, J., Ge, F., Zhang, B., Fu, X., Tomozawa, H., Sawashita, J., Mori, M, and Higuchi, K. 2010. Mouse senile amyloid fibrils deposited in skeletal muscle exhibit amyloidosis-enhancing activity. *PLoS Pathog*. 6: e1000914.

37. Saá, P., Yakovleva, O., de Castro, J., Vasilyeva, I., De Paoli, S.H., Simak, J., and Cervenakova, L. 2014. First demonstration of transmissible spongiform encephalopathy-associated prion protein (PrP^{TSE}) in extracellular vesicles from plasma of mice infected with mouse-adapted variant Creutzfeldt-Jakob disease by in vitro amplification. *J. Biol. Chem.* 289: 29247-29260.

38. Sawashita, J., Kametani, F., Hasegawa, K., Tsutsumi-Yasuhara, S., Zhang, B., Yan, J., Mori, M., Naiki, H., and Higuchi, K. 2009. Amyloid fibrils formed by selective N-, C-terminal sequences of mouse apolipoprotein A-II. *Biochim. Biophys. Acta.* 1794: 1517-1529.

39. Sawashita, J., Zhang, B., Hasegawa, K., Mori, M., Naiki, H., Kametani, F., and Higuchi, K. 2015. C-terminal sequence of amyloid-resistant type F apolipoprotein A-II inhibits amyloid fibril formation of apolipoprotein A-II in mice. *Proc. Natl. Acad. Sci. U S A.* 112: E836-845.

40. Sipe, J.D., Benson, M.D., Buxbaum, J.N., Ikeda, S., Merlini, G., Saraiva. M.J., and Westermark, P. 2016. Amyloid fibril proteins and amyloidosis: chemical identification and clinical classification International Society of Amyloidosis 2016 Nomenclature

Guidelines. *Amyloid* 23: 209-213.

41. Sponarova, J., Nyström, S.N., and Westermark. G.T. 2008. AA-amyloidosis can be transferred by peripheral blood monocytes. *PLoS One*. 3: e3308.

42. Xing, Y., and Higuchi, K. Amyloid fibril proteins. 2002. *Mech. Ageing Dev*. 123: 1625-1636.

43. Xing, Y., Nakamura, A., Chiba, T., Kogishi. K,. Matsushita, T., Li, F., Guo, Z., Hosokawa, M., Mori, M., and Higuchi, K. 2001. Transmission of mouse senile amyloidosis. *Lab. Invest.* 81: 493-499.

44. Xing, Y., Nakamura, A., Korenaga, T., Guo, Z., Yao, J., Fu, X., Matsushita, T, Kogishi, K., Hosokawa, M., Kametani, F., Mori, M., and Higuchi, K. 2002. Induction of protein conformational change in mouse senile amyloidosis. *J. Biol. Chem*. 277: 33164-33169.

45. Yan, J., Fu, X., Ge, F., Zhang, B., Yao, J., Zhang, H., Qian, J., Tomozawa, H., Naiki, H., Sawashita, J., Mori, M., and Higuchi, K. 2007. Cross-seeding and cross-competition in mouse apolipoprotein A-II amyloid fibrils and protein A amyloid fibrils. *Am. J. Pathol*. 171: 172–180.

46. Zhang, B., Une, Y., Fu, X., Yan, J., Ge, F., Yao, J., Sawashita, J., Mori, M., Tomozawa, H., Kametani, F., and Higuchi, K. 2008. Fecal transmission of AA amyloidosis in the cheetah contributes to high incidence of disease. *Proc. Natl. Acad. Sci. U S A.* 105: 7263-7268.

47. Zhang, H., Sawashita, J., Fu, X., Korenaga, T., Yan, J., Mori, M., and Higuchi, K. 2006. Transmissibility of mouse AApoAII amyloid fibrils: inactivation by physical and chemical methods. *FASEB J.* 20: 1012-1014.

Figure Legends

Fig. 1. Age-dependent increase in AApoAII amyloid deposition in donor mice. **(A)** AI of R1.P1-*Apoa2*^{c} mice that were injected with AApoAII amyloid fibrils at 2 months of age, and euthanized at the ages of 4, 6, 9 and 12 months (●), R1.P1-*Apoa2*^{c} mice without AApoAII injection (▼), and R1-*Apoa2*$^{-/-}$ mice without AApoAII injection (▲). Each symbol represents the AI of an individual mouse. Figures in parentheses indicate the numbers of amyloid-laden mice/numbers of mice examined. **(B)** Representative polarized light microscopic images of Congo red staining (*upper panels*) and bright-field light microscopic images of immunostaining with anti-APOA2 antiserum (*lower panels*). These images show the livers of 4 and 9-month-old R1.P1-*Apoa2*^{c} mice with induction of amyloidosis and 12-month-old R1.P1-*Apoa2*^{c} without induction. Scale bars = 100 μm.

Fig. 2. Comparison of AIA values of the WBC **(A)** and RBC **(B)** fractions collected from R1.P1-*Apoa2*^{c} mice (n = 3 in each point) with varying severities of AApoAII amyloidosis. Mice were induced amyloidosis at the age of 2 months and were euthanized at the ages of 4, 6, 9 and 12 months. Also, in the absence of induction, 12-month-old R1.P1-*Apoa2*^{c} mice (control) and 2-month-old R1-*Apoa2*$^{-/-}$ (*Apoa2*$^{-/-}$) mice were examined (n = 3 in each group). PBS: PBS-injected mice (n = 3). The AIA of each donor's cells was measured and (●) indicates the mean AIA of recipient mice. Bar indicates mean AIA of 3 donor mice. Significant differences between amyloidosis-positive and -negative mouse groups are indicated (#, $P < 0.05$; ##, $P < 0.01$; ###, $P < 0.001$. Kruskal-Wallis test followed by the Steel-Dwass test). **(C)** Representative polarized light microscopic images after Congo red

staining of the intestines and tongues of recipient mice that were administered the WBC fraction collected from the following donor animals: 4- and 9-month-old R1.P1-*Apoa2*^{c} mice with induction of amyloidosis and 12-month-old R1.P1-*Apoa2*^{c} mice without induction. Scale bars = 100 μm.

Fig. 3. Comparison of AIA values of plasmas collected from donor R1.P1-*Apoa2*^{c} mice (n = 3 in each point) with varying severities of AApoAII amyloidosis. Mice were induced amyloidosis at the age of 2 months and were euthanized at the ages of 4, 6, 9 and 12 months. Also, in the absence of induction, 12-month-old R1.P1-*Apoa2*^{c} mice (control) and 2-month-old R1-*Apoa2*$^{-/-}$ (*Apoa2*$^{-/-}$) mice were examined (n = 3 in each group). PBS: PBS-injected mice (n = 3). The AIA of each donor's plasma was measured and (●) indicate the mean AIA of recipient mice. Bar indicates the mean AIA of donor mice. **(B)** Representative polarized light microscopic images after Congo red staining of the intestines and tongues of recipient mice that were administered plasma collected from the following donor animals: 4- and 9- month-old R1.P1-*Apoa2*^{c} mice with induction of amyloidosis and 12-month-old R1.P1-*Apoa2*^{c} mice without induction. Scale bars = 100 μm.

Fig. 4. AIA of 3 fractions (3KG-P, 100KG-P and Sol) prepared from the pooled WBC and RBC fractions of 9-month-old AApoAII amyloid-laden R1.P1-*Apoa2*^{c} mice. Each bar shows the mean AIA of recipient mice in the group.

Fig. 5. A transmission electron microscopic image **(A)** and Western blotting images **(B** and C) of the 3 fractions of WBC fractions. **(A)** Amyloid fibril-like structures in the 3KG-P fraction of WBC fraction from 9-month-old AApoAII amyloid-laden R1.P1-*Apoa2*^{c} mice are indicated by arrows. Scale bar = 100 nm. **(B and C)** Western blotting images with anti-APOA2 antiserum of the 3 fractions of WBC fraction collected from 9-month-old AApoAII amyloid-laden R1.P1-*Apoa2*^{c} **(B)** and 2-month-old R1-*Apoa2*$^{-/-}$ mice **(C)**. 0.5 μg AApoAII in **(B and C)** and 1 μL plasma in **(B)** of 2-month-old R1.P1-*Apoa2*^{c} mouse were used as positive references. The specific bands at ~7 kDa (monomer) and ~15 kDa (dimer) in 3KG-P are indicated by white circles in (**B**).

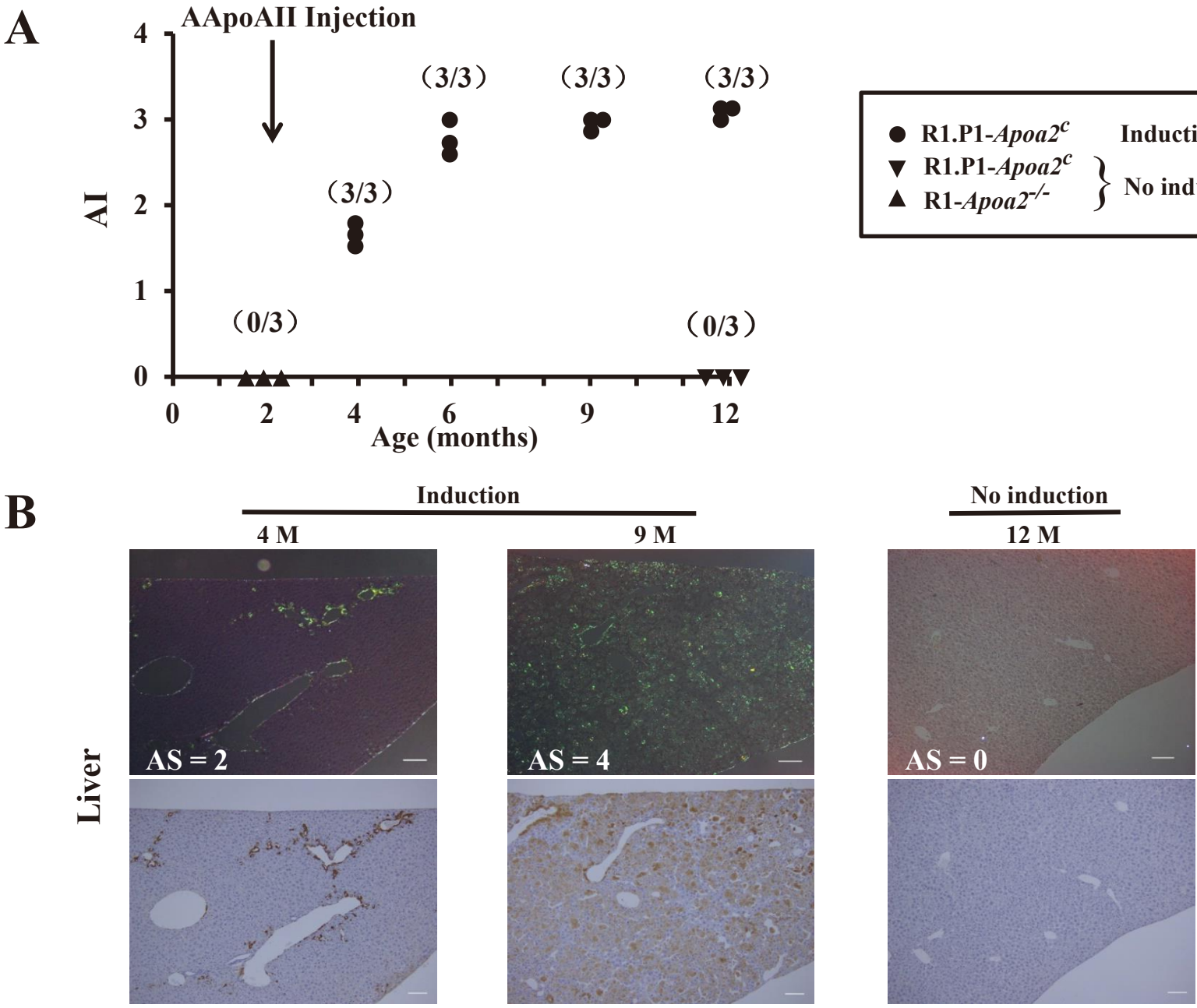
A
AApoAII Injection
AI
Age (months)
(3/3)
(3/3)
(3/3)
(3/3)
(0/3)
(0/3)
R1.P1-Apoa2c
R1.P1-Apoa2c
R1-Apoa2-/-
Inducti
No ind
B
Induction
No induction
4 M
9 M
12 M
Liver
AS = 2
AS = 4
AS = 0

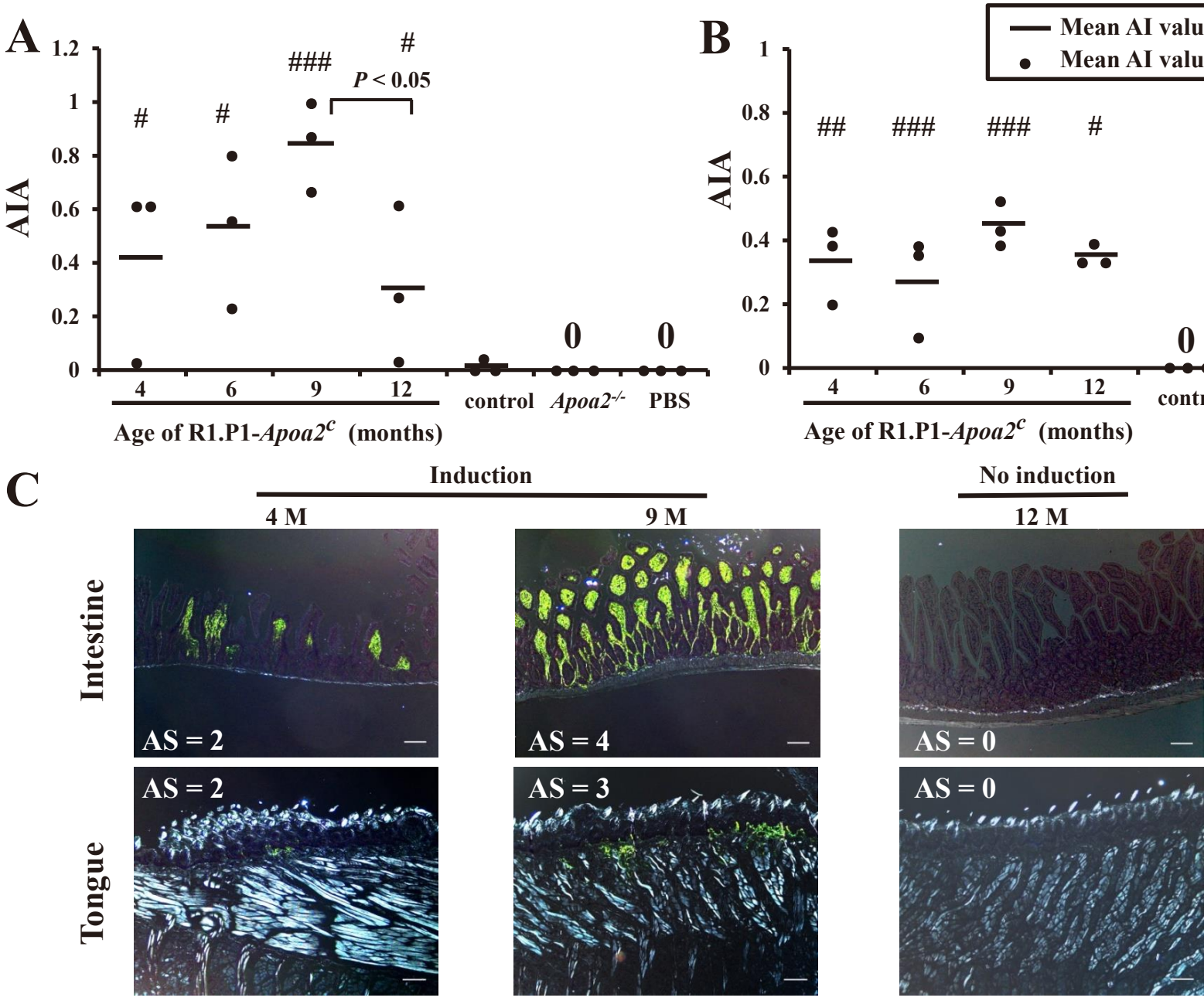
A
AIA
1.2
1
0.8
0.6
0.4
0.2
0
#
#
###
#
P < 0.05
0
0
4
6
9
12
control
Apoa2-/-
PBS
Age of R1.P1-Apoa2c (months)
B
Mean AI valu
Mean AI valu
AIA
1
0.8
0.6
0.4
0.2
0
##
###
###
#
0
4
6
9
12
Age of R1.P1-Apoa2c (months)
C
Induction
No induction
4 M
9 M
12 M
Intestine
Tongue
AS = 2
AS = 4
AS = 0
AS = 2
AS = 3
AS = 0

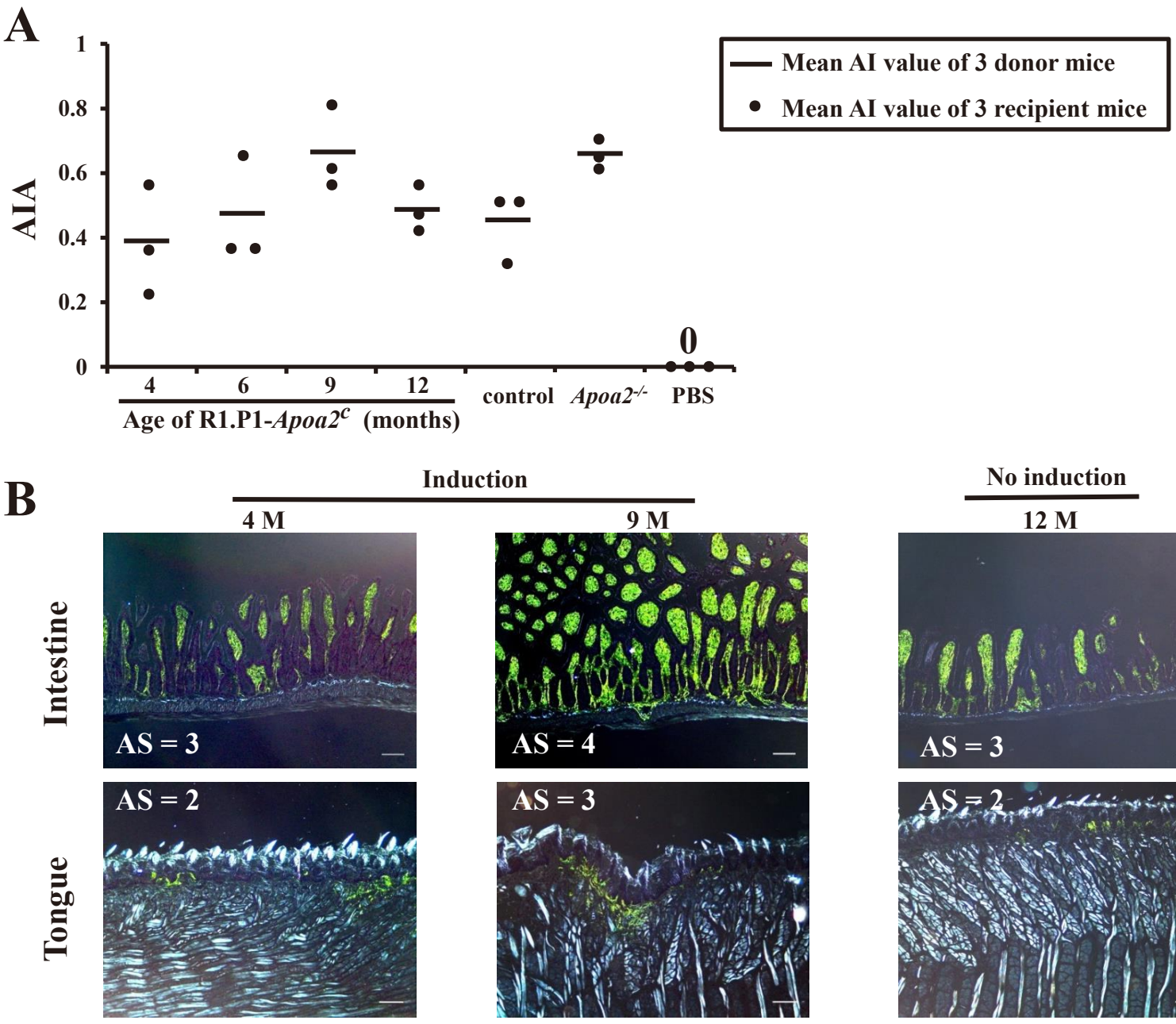
A
1
0.8
0.6
0.4
0.2
0
AIA
Mean AI value of 3 donor mice
Mean AI value of 3 recipient mice
0
4
6
9
12
control
Apoa2-/-
PBS
Age of R1.P1-Apoa2c (months)
B
Induction
No induction
4 M
9 M
12 M
Intestine
Tongue
AS = 3
AS = 4
AS = 3
AS = 2
AS = 3
AS = 2

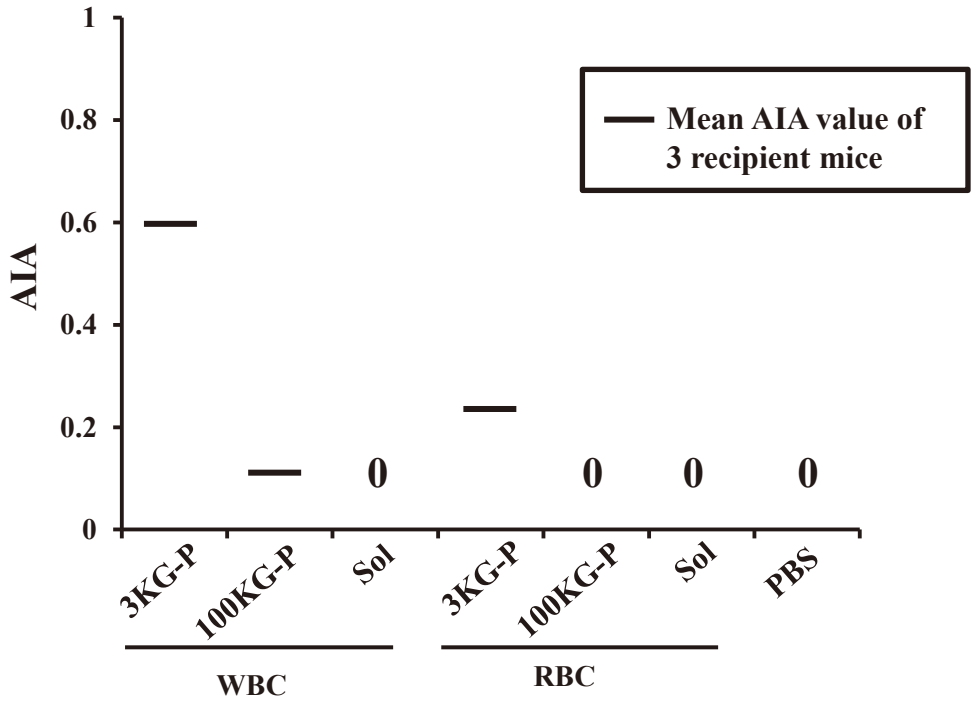
1
0.8
0.6
0.4
0.2
0
AIA
Mean AIA value of
3 recipient mice
0
0
0
0
3KG-P
100KG-P
Sol
3KG-P
100KG-P
Sol
PBS
WBC
RBC

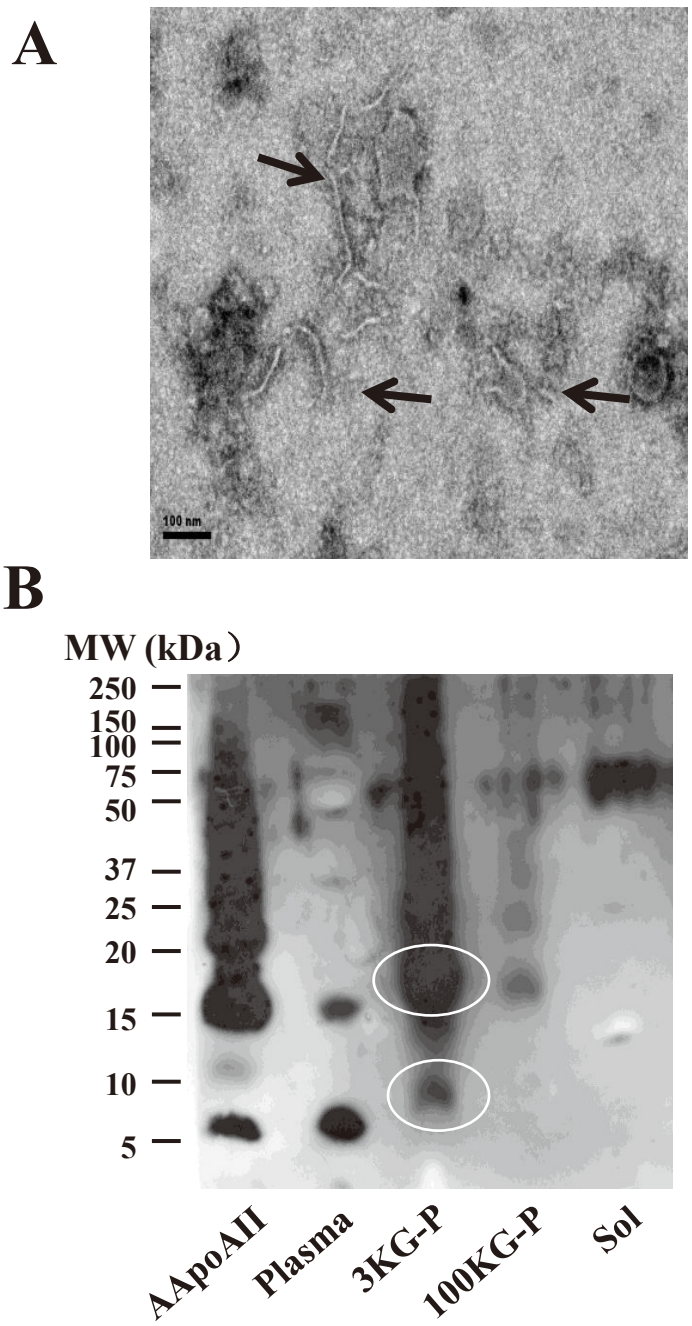
A
100 nm
B
MW (kDa）
250
150
100
75
50
37
25
20
15
10
5
AApoAII
Plasma
3KG-P
100KG-P
Sol
C
MW (kDa）
250
150
100
75
50
37
25
20
15
10
5
AApoAII
3KG-P
100KG-P

Table 1 Cell numbers contained in 20 μL WBCs and RBCs suspensions injected into recipient 2-month-old R1.P1-*Apo*

Donor group	Injection	
	WBCs ($\times 10^7$)	RBCs ($\times 10^7$)
4 M R1.P1-*Apoa2*^{c} + AApoAII	0.46 ± 0.10	6.15 ± 1.48
6 M R1.P1-*Apoa2*^{c} + AApoAII	0.49 ± 0.06	6.53± 0.65
9 M R1.P1-*Apoa2*^{c} + AApoAII	0.49 ± 0.08	4.64 ± 0.70
12 M R1.P1-*Apoa2*^{c} + AApoAII	0.43 ± 0.09	3.40 ± 0.38
12 M R1.P1-*Apoa2*^{c}	0.46 ± 0.05	5.22 ± 0.24
2 M SAMR1.*Apoa2*$^{-/-}$	0.50 ± 0.07	6.42 ± 1.08

WBCs and RBCs were isolated from 3 mice in each group and cell numbers were calculated. WBCs and RBCs samples diluted with PBS to 100 μL and injected into the tail vein of 3 recipient R1.P1-*Apoa2*^{c} mice.

Table 2 Amyloidosis-inducing activities (AIA) of denatured WBCs, RBCs and plasma samples.

Injection	No. of mice (n)	Mean AIA	No. of positive mice (positive/total)
WBCs	3	0	0/3
RBCs	6	0	0/6
Plasma	6	0	0/6

The denatured samples containing the same amount of protein in 20 μL of the original pooled sample were injected into recipient R1.P1-*Apoa2*^{c} mice.

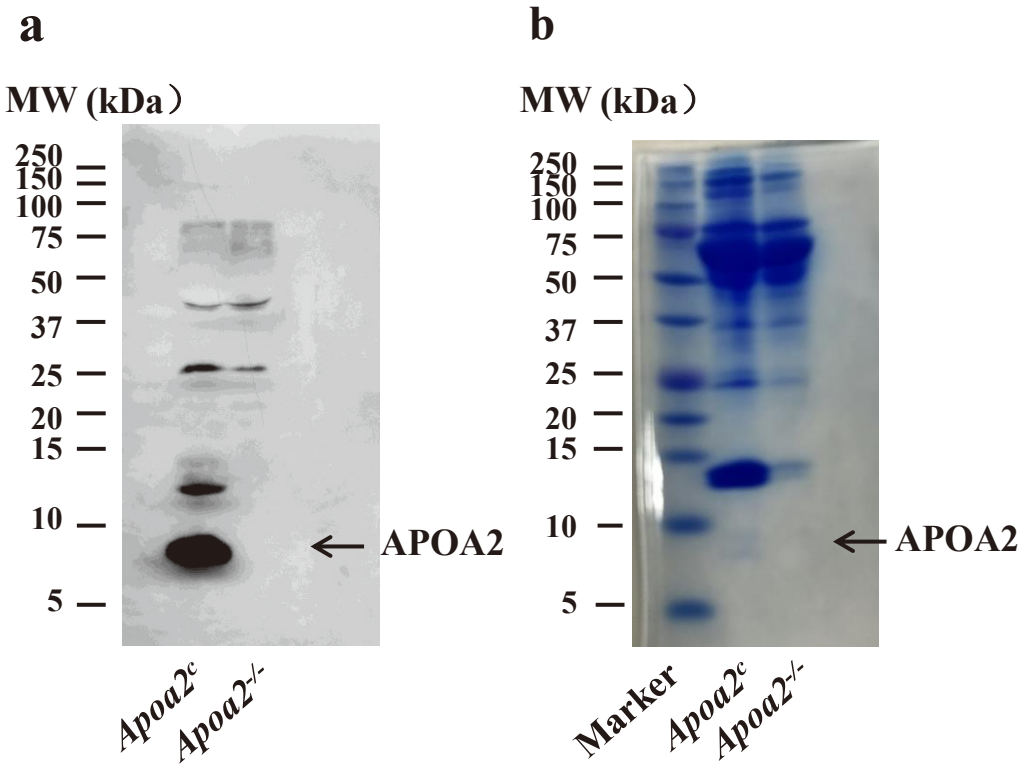

Fig. S1. Western blotting **(a)** and CBB staining **(b)** of 1 µl plasma from R1.P1-*Apoa2*^{c} a
R1-*Apoa2*$^{-/-}$ mice. Western blotting and CBB staining were performed with 16.5% SDS-
PAGE and membrane was incubated with polyclonal rabbit anti-mouse APOA2 antiseru
[14] in Western blotting.

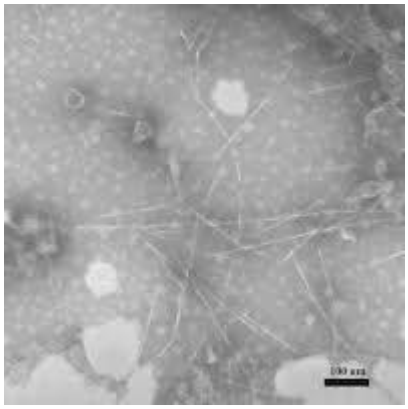

Fig. S2. A negatively stained electron microscopic image of AApoAII amyloid fibril fraction isolated from the livers of amyloidosis induced 13-month-old R1.P1-*Apoa2*^{c} mice. Scale bar = 100 nm.

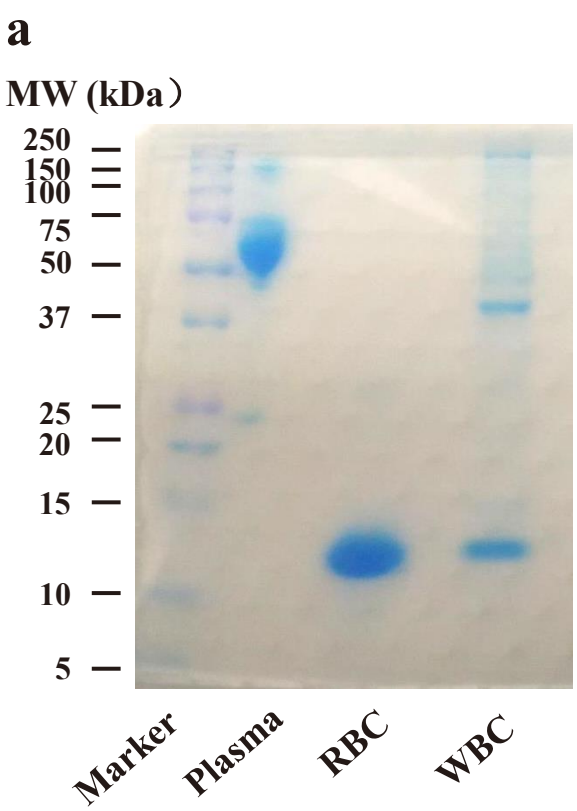

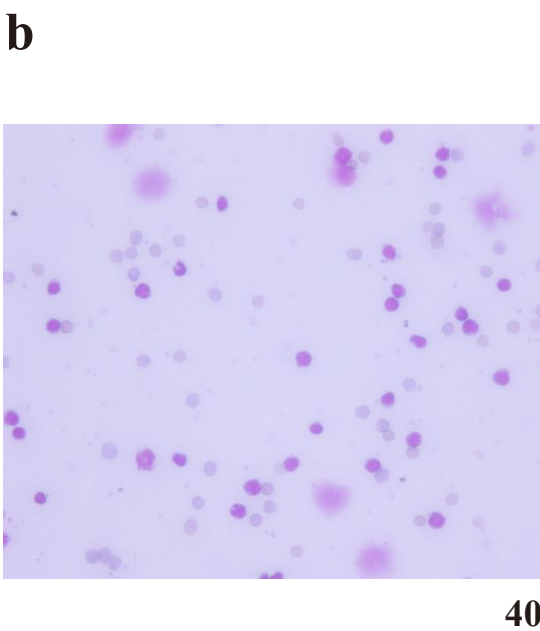

Fig. S3. CBB staining of 0.25 µl plasma, 10 µg RBC and 10 µg WBC fractions from R1.P1-*A*
mice separated with 10% SDS-PAGE **(a)**. Smear prepared by an auto-smearing device (Cytosp
Shandon Scientific Ltd., Cheshire, UK) of the WBC fractions were stained with May-Giemsa

Table S-1 Injected protein amounts of the pooled WBC and RBCs suspensions into recipient mice.

Samples	Injected protein amounts（μg）
3KG-P of WBCs	38
100KG-P of WBCs	35
Soluble of WBCs	70
3KG-P of RBCs	30
100KG-P of RBCs	140
Soluble of RBCs	530

Samples corresponding to 20 μl volume of original pooled RBCs and WBC suspensions were injected into 3 recipient R1.P1-*Apoa2*^{c}